

Cleavage of The Double-strand Region in Alkali-denatured Supercoiled Plasmid pBR322 Leads to DNA Nodes*

TIAN Lei¹⁾, SU Xiao-Yun²⁾, ZHANG Zhen-Feng^{3)**}, HUANG Xi-Tai⁴⁾

¹⁾ Department of General Surgery, Navy General Hospital, Beijing 100048, China;

²⁾ Key Laboratory for Feed Biotechnology of The Ministry of Agriculture, Feed Research Institute, Chinese Academy of Agricultural Sciences, Beijing 100081, China;

³⁾ State Key Laboratory of Microbial Resources, Institute of Microbiology, Chinese Academy of Sciences, Beijing 100101, China;

⁴⁾ Department of Biochemistry and Molecular Biology, College of Life Sciences, Nankai University, Tianjin 300071, China)

Abstract Combinatorial analyses including enzymatic analysis and atomic force microscopy (AFM) were used to gain more insights into structure of the alkali-denatured plasmid pBR322 DNA (DNA IV). Among the restriction enzymes tested, *Pst* I was able to cleave the pBR322 DNA IV molecules, indicative of the existence of an intact restriction site in the denatured DNA. AFM images revealed that *Pst* I-treated DNA IV molecules contained an individual node. The contour length of the condensed molecules was decreased by about 11% compared to DNA IV. Intriguingly, the *Escherichia coli* topoisomerase IV, a type II topoisomerase, also introduced nodes into DNA IV while keeping the molecules in a closed form. The two types of DNA were similar to each other in terms of the contour length and the size of the node based on the AFM analysis. These findings suggest that specific base-paired regions exist in DNA IV, and that cleavages at these regions may lead to DNA node.

Key words DNA IV, restriction enzyme, DNA topoisomerase, DNA nodes, atomic force microscopy (AFM)

DOI: 10.16476/j.pibb.2015.0160

DNA is the most important genetic material of the cellular organisms. The structure of DNA has great effects on its functions in cells. A double-stranded DNA molecule has been demonstrated to be one of the three structural forms: supercoiled DNA (DNA I), relaxed or open circular DNA (DNA II) and linear DNA (DNA III)^[1-2]. The DNA molecules in prokaryotic cells, including the chromosomal DNA and the extrachromosomal genetic elements, are usually in the form of DNA I. The superhelical state of intracellular DNA is thus an important structural determination of DNA functions^[3-4].

DNA denaturation is induced by breaking the hydrogen bonds of the base pairs between the strands^[5]. DNA denaturation serves an essential role in many cellular processes, which require the separation of the DNA double strands. A prominent example is the local denaturation of the origin site during the initiation of

DNA replication by DnaA in bacteria^[6] or by RPA in eukaryotes^[7]. In cells, binding of a site specific protein^[8] or high level of negative supercoiling^[6, 9] also induce local denaturation of DNA. Abiotically, DNA can be denatured by stretching^[10-11], thermal treatment^[12], and chemical denaturants, including alkali^[13]. At a high pH point, the supercoiled DNA can be denatured into a stable structure, which is termed alkali-denatured supercoiled DNA (DNA IV). DNA IV had been considered to be an irreversibly denatured structure, existing as the randomly coiled form of circular DNA^[14]. However, this argument might not be true as

*This work was supported by grants from The National Natural Science Foundation of China (31270124, 30900023).

**Corresponding author.

Tel: 86-10-64807418, E-mail: zhangzff@im.ac.cn

Received: April 5, 2016 Accepted: May 16, 2016

the denatured supercoiled DNA was then demonstrated to be renatured rapidly under precisely controlled conditions, including pH, temperature and ion strength^[15-16]. Many research efforts have also been made in studying the structure of DNA IV. In early studies, the conformation of bacteriophage Φ X174 DNA in form IV was determined by transmission electron microscopy. The Φ X174 DNA IV molecules showed supercoiling appearance with protrusions, the total contour length of which was approximately half of that of the relaxed DNA^[17-18]. Recently, the alkali-denatured supercoiled pBR322 DNA was visualized by atomic force microscopy (AFM)^[13]. The high quality images provided more structural details about the DNA IV molecules. In contrast to the Φ X174 DNA IV, the denatured pBR322 DNA is circular without any visible supercoiled turns. In addition, the topologically linked strands showed rough surfaces due to the kink structures.

In the present work, the plasmid pBR322 form *E. coli* was employed to study the alkali denaturation of DNA. The results showed that pBR322 DNA IV could be cleaved by *Pst* I, a restriction enzyme, to form a knotted structure. Further analysis showed that the *E. coli* Topo IV, a type II topoisomerase, also converted pBR322 DNA IV into a novel type structure containing DNA node. The contour lengths of both structures were decreased significantly compared to DNA IV. Our results strongly support the argument that DNA IV contains natural double-stranded regions. And, the findings that cleavage of the double-strand region induced nodes of DNA IV may shed light on the studies of DNA in complicated conformations.

1 Materials and methods

1.1 Preparation of plasmid DNA samples

The plasmid pBR322 (4 361 bp) was transformed into *Escherichia coli* strain HB101 (*recA*13, *topA*⁺). Plasmid isolation and purification were performed as described previously^[2]. Plasmid DNA samples were treated by 0.2 mol/L NaOH solution for 15 min at room temperature for completely denaturation. The alkali-treated plasmid DNA was then neutralized with equal volume of 0.2 mol/L HCl solution and recovered using QIAquick PCR Purification Kit (Qiagen, Germen).

1.2 Restriction enzyme assays

All the restriction enzymes were purchased from NEB (Ipswich, USA). The DNA samples (0.1 μ g)

were mixed with 1 U of each of the enzymes respectively in the corresponding 1 \times reaction buffer to a final volume of 10 μ l. Reactions were performed at 37 °C for 1 h and stopped by adding 2 μ l 6 \times loading dye containing 60 mmol/L EDTA and 0.6% SDS. The DNA samples were then analyzed by 1-D agarose gel electrophoresis as describe below.

1.3 Topoisomerase assays

The *E. coli* DNA topoisomerase IV was purchased from TopGen (Port Orange, USA). Unless otherwise noted (as in Figure 3b), reactions contained the followings (20 μ l): 0.2 μ g DNA, 1 U Topo IV, 40 mmol/L Tris-HCl (pH 7.5), 6 mmol/L MgCl₂, 10 mmol/L DDT, 100 mmol/L potassium glutamate, 40 μ mol/L ATP and 50 mg/L BSA. Reactions were terminated after 30 min at 37 °C with SDS (1%) followed by proteinase K digestion (50 mg/L, 15 min at 50 °C). The DNA samples were then analyzed by 1-D or 2-D agarose gel electrophoresis.

1.4 Agarose gel electrophoresis

For 1-D gel electrophoresis, DNA samples were loaded onto 1% agarose gel in 1 \times TAE buffer in the presence of 0.5 mg/L ethidium bromide (EB) for 1.5 h at a voltage of 6 V/cm. The gel was then photographed with GDS-8000 system, UVP. 2-D gel electrophoresis was performed to analyze the topology of DNA samples. Briefly, the samples were loaded onto 1% agarose gel in 1 \times TAE buffer in the presence 1 mg/L chloroquine for 12 h at a voltage of 2 V/cm for the 1st-dimensional electrophoresis. Then, the gel was soaked in 1 \times TAE buffer containing 5 mg/L chloroquine for over 6 h. After the gel was turned 90°, the 2nd-dimensional electrophoresis was performed in the same buffer for 4 h at a voltage of 3 V/cm. The gel was soaked in 1 mmol/L MgCl₂ solution to elute the chloroquine and stained with EB. The photographs of the gel were then captured with GDS-8000 system, UVP.

1.5 Atomic force microscopy

The bands corresponding to different DNA forms of pBR322 were cut out from the agarose gel in the absence of EB and the DNAs were purified by the Gel and PCR Clean-Up System (Promega Co., Madison, WI, USA). The purified DNAs were dissolved in nuclease free water. To adsorb plasmid DNAs onto the mica substrate, MgCl₂ was added to each sample solution to a final concentration of 2 mmol/L. A 10 μ l drop of the DNA sample (5 μ g/L) was deposited on the freshly cleaved mica and allowed to stand for

5 min at ambient. The sample was then rinsed with 100 μ l aliquots of distilled deionized water for 3 times and dried for 4 min in a weak stream of nitrogen.

Tapping mode AFM was performed using a Nanoscope III a Multimode-AFM instrument (Digital Instruments, Santa Barbara, CA) under ambient conditions. Super-sharp silicon tips (Silicon-MDT Ltd., Moscow, Russia) with resonance frequency of about 246 kHz were used at a scan rate of 1~2 Hz. Once the tip was engaged, the set point value was adjusted to minimize the force exerted on the sample while maintaining the sharpness of the image.

Length measurements of DNA molecules were performed manually using the software ImageJ (Wayne Rasband, National Institute of Health, USA). Diameter and height measurements of DNA strands or nodes were performed manually using the software provided with the Nanoscope instrument. 45 or up to 100 molecules were chosen to be analyzed for different samples. Mean values were obtained by fitting to a Gaussian curve.

2 Results and discussion

2.1 Restriction analysis of pBR322 DNA IV

To detect whether the double-stranded regions exist in the alkali-denatured supercoiled pBR322 plasmid DNA, selected restriction enzymes (*Bam*H I, *Ava* I, *Nde* I, *Pst* I, and *Eco*R I) were used individually to treat pBR322 DNA IV. As shown in

Figure 1a, all enzymes can theoretically introduce a single site cleavage of the DNA double strands in the intact pBR322. The GC% of the restriction sites are 33% for *Eco*R I and *Nde* I, 67% for *Bam*H I and *Pst* I, and 83% for *Ava* I respectively. The restriction digested products were then subjected to agarose gel electrophoresis and the results were shown in Figure 1b. DNA IV (DS band, lane 2) ran much faster than DNA I in the gel (SC band, lane 1). Despite the existence of linear DNA generated from the small amounts of the supercoiled DNA in the sample, most enzymes appeared to have no significant effects on the electrophoretic behavior of DS IV (lanes 3, 4, 6 and 7), suggesting the failure of these enzymes in cutting the strands of DNA IV. The explanation would be that the restriction sites in pBR322 DNA IV for these enzymes were impaired by alkali-treatment, hence not recognizable by them. Intriguingly, however, *Pst* I treatment induced a significant change in the electrophoresis behavior of alkali-treated pBR322. As could be seen in Figure 1b, the sharp DS band disappeared; instead, a smear above the DS band appeared in the *Pst* I-treated sample, suggesting that the heterogeneity in the structure of such DNA. Notably, *Pst* I treatment of DNA IV did not induce either renaturation of DNA or separation of the DNA strands since the position of the smear on the gel was far from those of the linear pBR322 DNA (Figure 1b, lane 9) or of the single-stranded pBR322 DNA (Figure 1b, lane 8).

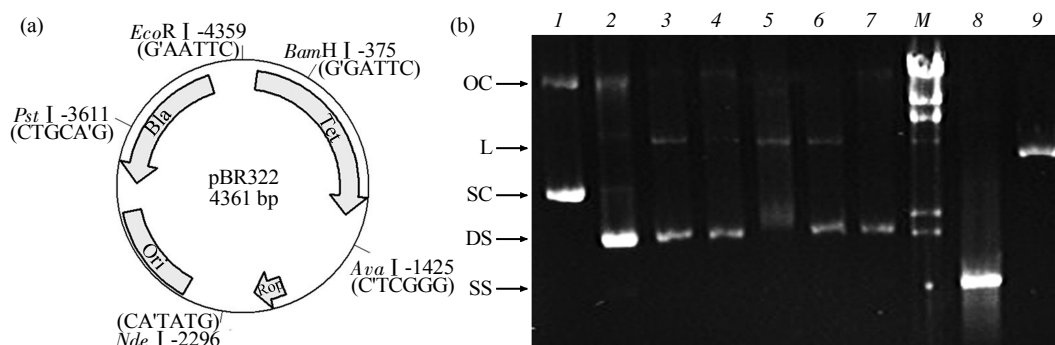


Fig. 1 Restriction enzyme analysis of alkali-denatured supercoiled pBR322 DNA

(a) Map of plasmid pBR322 DNA with the sites for selected restriction enzymes and the corresponding recognition sequence labeled. (b) Agarose gel electrophoresis of the plasmid pBR322. Lane 1, control; lane 2, alkali denatured pBR322; lane 3~7, denatured pBR322 digested by *Eco*R I (lane 3), *Bam*H I (lane 4), *Pst* I (lane 5), *Nde* I (lane 6) and *Ava* I (lane 7), respectively; lane 8, linear single-stranded DNA; lane 9, pBR322 linearized by *Pst* I; M, DNA molecular mass marker. OC, open circular DNA (DNA II); L, linear DNA (DNA III); SC, supercoiled DNA (DNA I); DS, denatured supercoiled DNA (DNA IV); SS, single-stranded DNA.

To learn more about the structural changes induced by *Pst* I treatment, the purified *Pst* I-treated

DNA IV and the DNA samples in other forms were all visualized by AFM and compared (Figure 2). As

shown in Figure 2a, the supercoiled DNA molecules adopted a plectonemical structure, with the supercoiling level of individual molecules different from each other. *Pst* I treatment of the supercoiled DNA generated homogenous linear pBR322 DNA molecules (Figure 2b). No obvious special structure was found in these molecules, indicating that *Pst* I did not introduce any higher structure into the DNA. DNA IV molecules were still circular, with rough surface and shortened contour length (Figure 2c) compared with the supercoiled DNAs. The structure of DNA IV, however, changed greatly after treatment by *Pst* I (Figure 2d). The DNA molecules were all converted into open forms. Two DNA strands with free ends were observed in most molecules (white arrows in

Figure 2d~f), suggesting that *Pst* I cleaved both strands of DNA IV at a single site. Since *Pst* I can only bind to and cleave its restriction site, the *Pst* I site in pBR322 DNA IV must remain in intact double helix with perfect base pairing. Moreover, most of the molecules contained an intramolecular condensed DNA structure with variable diameters. Judging from the rugged surface of this structure, it might be an assembly of several DNA nodes. DNA loops and strands in each molecule surrounded the condensed structure. Only one loop was observed in about half of the molecules (Figure 2e), while up to three loops were found in some other molecules (Figure 2f). The lengths of the strands with free end were varied, indicating the DNA nodes might slip along the DNA strands.

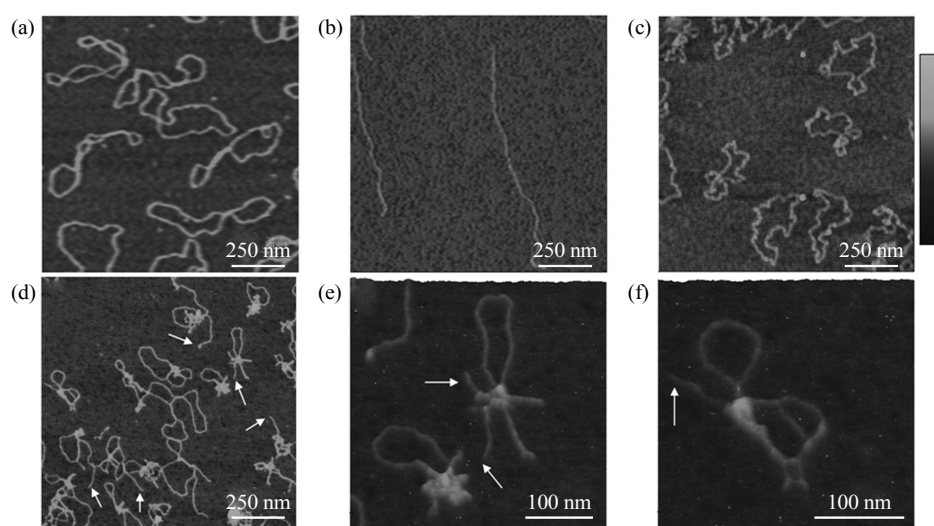


Fig. 2 AFM images of pBR322 DNA in different forms

(a) Supercoiled DNA (DNA I). (b) Linear DNA (DNA III). (c) Alkali-denatured supercoiled DNA (DNA IV). (d) DNA IV digested by *Pst* I (DNA V). (e) and (f) 3-D view of the representative molecules of DNA V selected from (d). The grayscale represents 5 nm.

Treatment of denatured supercoiled Φ X174 DNA with single-strand specific nucleases could lead to reversion of the separated strands into natural DNA duplex [15]. By contrast, we show here that the double-strand break (DSB) introduced by *Pst* I into pBR322 DNA IV caused DNA condensation rather than renaturation. The striking differences in the responses of DNA IV to nick and DSB prompted us to speculate that the double-stranded regions in DNA IV might serve an essential role in DNA renaturation. When nicks in single strands occur, the twisting force restrained in the denatured supercoiled DNA may

drive the strands shift with each other for base pairing, as the strands are locked at the double helix regions all through the renaturation process. On the contrary, once the double-strand is broken, the instantaneous release of the twisting force in both strands may result in random movement of the strands and substantial formation of nodes in the DNA.

2.2 Topoisomerase assays of pBR322 DNA IV

DNA topoisomerases were then used to treat pBR322 DNA IV to investigate whether the superhelical strength restrained in the molecules could be relaxed. DNA gyrase and Topo IV from *E. coli*, two

types of type II topoisomerase that cut both strands simultaneously, were used in the assays. Gyrase had no perceivable effects on DNA IV in the presence or absence of ATP (data not shown), while Topo IV obviously changed the structure of DNA IV (Figure 3). The results of 2-D gel electrophoresis showed that Topo IV efficiently relaxed the supercoiled DNA (compare lane 1 and 2 in Figure 3). Under our experiment condition, the relaxed DNA appeared to be slightly positively supercoiled in the 2-D agarose gel electrophoresis. In contrast, the DNA IV pBR322 plasmid could not be relaxed by Topo IV. The Topo IV-

treated DNA IV appeared to be a mixture of dispersed bands, migrating faster in both dimensions than the supercoiled DNA (Figure 3, lane 4). The requirements for Topo IV catalyzing structural changes of DNA IV were then analyzed (Figure 3b). In the absence of Mg^{2+} , Topo IV had no effects on DNA IV (compare lanes 7, 8 to lane 5 in Figure 3b). Although Mg^{2+} alone could stimulate a moderate structural transition of DNA IV by Topo IV in the absence of ATP (Figure 3b, lane 6), ATP was required for efficient reaction (Figure 3b, lane 5).

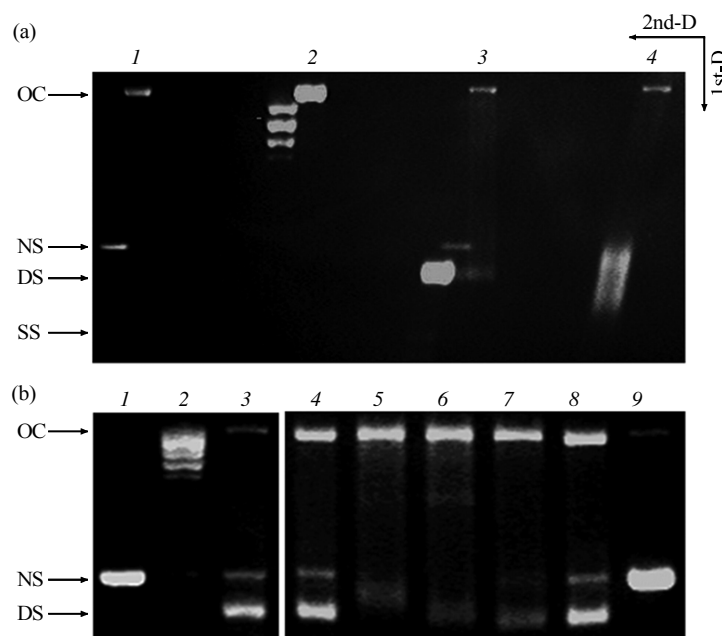


Fig. 3 Agarose gel electrophoresis of the denatured or non-denatured supercoiled pBR322 DNA treated by Topo IV

(a) 2-D agarose gel electrophoresis of the denatured or non-denatured supercoiled pBR322 DNA treated by topoisomerase IV (Topo IV) from *E. coli*. Lane 1, untreated pBR322; lane 2, Topo IV treated pBR322; lane 3, alkali-denatured pBR322; lane 4, Topo IV treated alkali-denatured pBR322. OC, open circular DNA or relaxed circular DNA (DNA II); NS, negatively supercoiled DNA; DS, denatured supercoiled DNA (DNA IV); SS, single-stranded DNA. The dimensions of the electrophoresis were also labeled. (b) Topo IV catalyzes structural transition of denatured pBR322 progressively in the presence of Mg^{2+} and ATP. Lanes 1 and 9, untreated pBR322; lane 2, pBR322 relaxed by Topo IV; lanes 3 and 4, alkali-denatured pBR322; lane 5, Topo IV treated alkali-denatured pBR322 in the presence of 2 mmol/L Mg^{2+} and 1 mmol/L ATP; lane 6, Topo IV treated alkali-denatured pBR322 in the presence of 2 mmol/L Mg^{2+} ; lane 7, Topo IV treated alkali-denatured pBR322 in the presence of 5 mmol/L EDTA and 1 mmol/L ATP; lane 8, Topo IV treated alkali-denatured pBR322 in the presence of 5 mmol/L EDTA. OC, open circular DNA or relaxed circular DNA (DNA II); NS, negatively supercoiled DNA; DS, denatured supercoiled DNA (DNA IV).

The Topo IV-treated DNA samples were further visualized by AFM (Figure 4). Figure 4a, b (Figure 4b is a zoom-in view of Figure 4a) showed that Topo IV converted the supercoiled DNA into completely relaxed structure without any residual supercoils or newly formed structures. In contrast, for DNA IV,

Topo IV treatment induced significant DNA nodes while keeping the molecules still closed (Figure 4c, d, Figure 4d is a zoom-in view of Figure 4c). DNA loops in apparently different diameters were observed to extend from the central condensed structure. One relatively long loop was always observed, which was

associated with 2 ~3 short loops for each DNA molecule. A comparison of the DNA molecules in Figure 2f and Figure 4d showed that the structures of the DNA nodes of pBR322 DNA IV treated by Topo IV or *Pst* I are similar. Topo IV has been reported to be able to knot DNA in a low efficiency^[19]. And the knotted structure of plasmid DNA catalyzed by Topo IV *in vivo* was demonstrated by AFM^[20]. However, the loosely knotted DNA was quite different from the condensed DNA observed in the present work. Moreover, much evidence has demonstrated that Topo IV

prefers to unknot DNA both *in vitro* and *in vivo*^[21-22]. Considering the high efficiency of DNA IV conversion into knotting-like structures in our experiment, the possibility that Topo IV catalyzed knotting of DNA IV directly could be ignored. The mechanism of DNA structural transition induced by Topo IV might be similar to that induced by *Pst* I. Once the DSB was introduced by Topo IV into DNA IV, release of the twisting force drove the formation of DNA nodes, and the strands were then re-ligated by Topo IV.

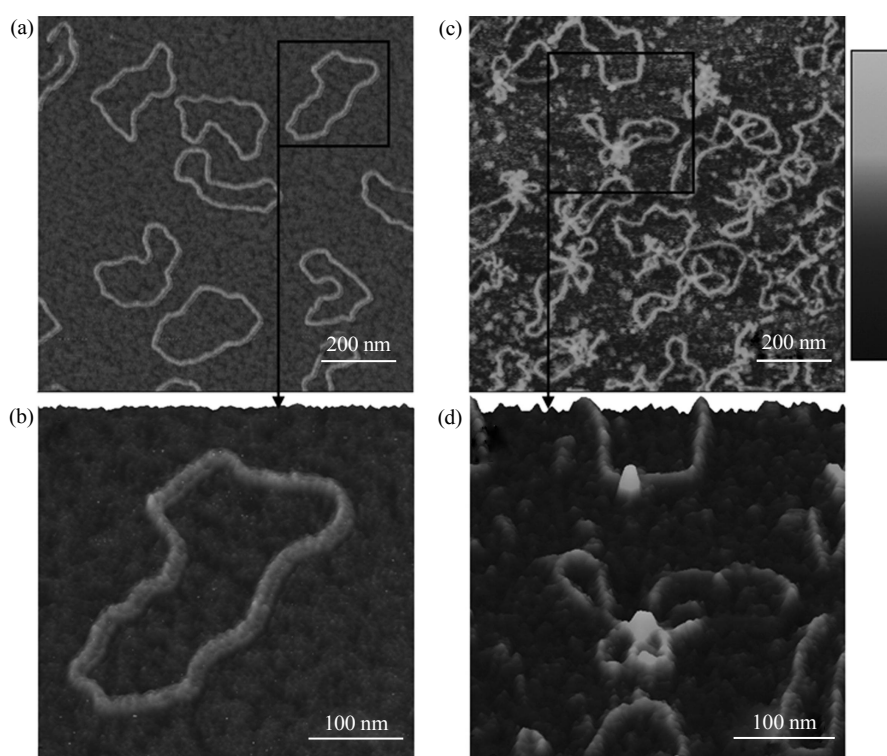


Fig. 4 AFM images of pBR322 DNA I and DNA IV treated by *E. coli* Topo IV

(a) Relaxed DNA (DNA II) produced by Topo IV. (b) A zoom-in 3-D image of the selected area in (a). (c) Topo IV-treated DNA IV. (d) A zoom-in 3-D image of the selected area in (c). The grayscale represents 3 nm.

The size of binding site for Topo IV on DNA was about 30 bp^[23]. Therefore, one would expect that the size of one of the double-stranded regions will be no less than this value. For DNA gyrase, more than 130 bp are required for its efficient binding to DNA^[24]. Therefore, the failure of gyrase to affect the structure of DNA IV might be ascribed to the insufficient length of the double-stranded region.

2.3 Structural comparison of pBR322 DNA in different forms

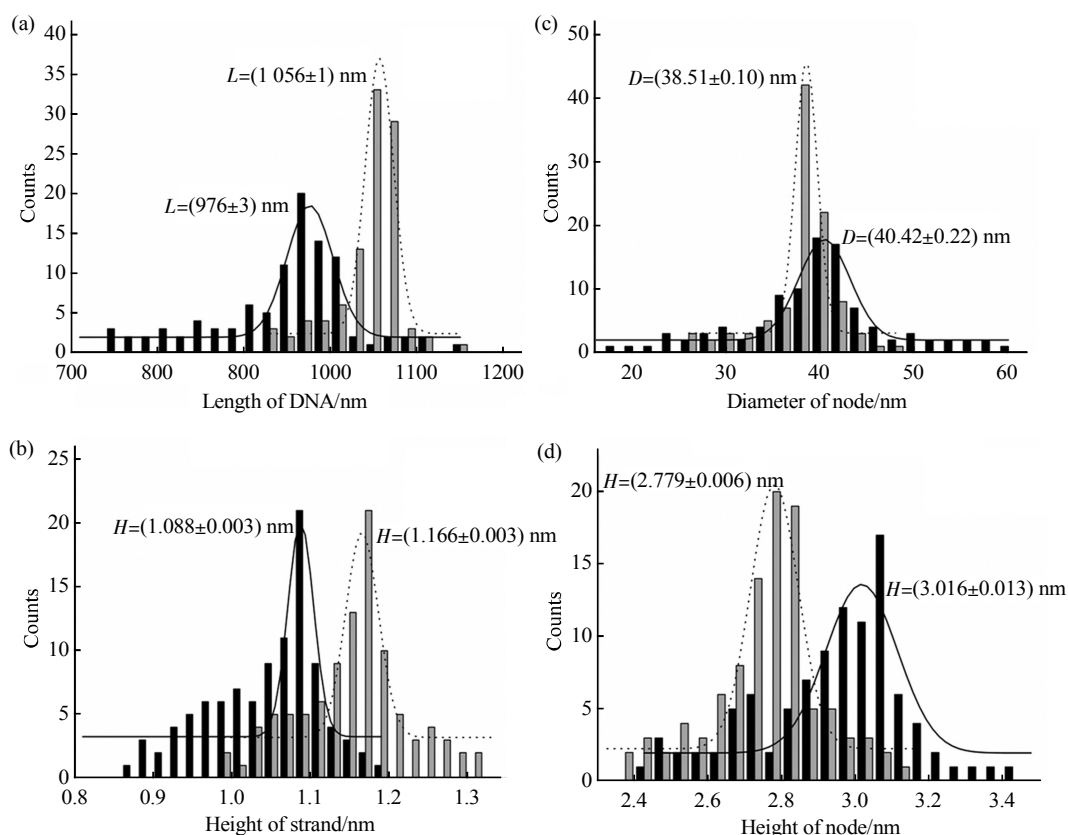
Structural parameters of 45 or up to 100 DNA

molecules for different DNA forms were measured manually. The mean values of the apparent length and height of the DNA double-strands for the supercoiled, relaxed, linear or denatured DNA molecules were calculated by averaging the 45 values measured (Table 1, see data for DNA I ~ IV respectively). Meanwhile, the structural parameters for DNA V and DNA VI, including the length and height of DNA strands as well as the diameter and height of the nodes, were obtained by processing the data sets statistically as shown in Figure 5. All the DNA forms showed a similar height

Table 1 Comparison of the structural parameters of plasmid pBR322 DNA molecules in different conformations

| pBR322 | Number of molecules | Contour length/nm | Height of strands/nm | Diameter of the node/nm | Height of the node/nm |
|----------------------|---------------------|-------------------|----------------------|-------------------------|-----------------------|
| DNA I | 45 | (1412 ± 8) | (0.97 ± 0.04) | – | – |
| DNA II | 45 | (1414 ± 5) | (0.92 ± 0.03) | – | – |
| DNA III | 45 | (1406 ± 16) | (1.02 ± 0.04) | – | – |
| DNA IV | 45 | (1180 ± 9) | (1.15 ± 0.05) | – | – |
| DNA V ¹⁾ | 100 | (976 ± 3) | (1.088 ± 0.003) | (40.42 ± 0.22) | (3.016 ± 0.013) |
| DNA VI ¹⁾ | 100 | (1056 ± 1) | (1.166 ± 0.003) | (38.51 ± 0.10) | (2.779 ± 0.006) |

¹⁾ The data shown here was correspond to that in Figure 5.

**Fig. 5 Distribution of the corresponding structure parameters measured for DNA V and DNA VI molecules**

The normalized histograms of the apparent counter length (a), height of DNA strands (b), diameter of DNA nodes (c) and height of DNA nodes (d) of DNA V and DNA VI with Gaussian fit are shown. The fitting curves are shown in solid lines for DNA V and in dot lines for DNA VI with the mean value for each parameter labeled. ■: DNA V; ▒: DNA VI.

of strands, suggesting that the strands kept intertwined with each other during the structural transformations. Nevertheless, the lengths of different DNA forms largely varied. Compared to the length of the supercoiled DNA (~1 412 nm), an unchanged apparent contour length of DNA II (~1 414 nm) and DNA III (~1 406 nm) was observed, suggesting that relaxation or linearization had little effects on the length of DNA. By contrast, the contour length of

DNA IV (~1 180 nm) was decreased by about 16%, a value nearly identical to that reported in our previous work^[13]. Notably, the *Pst* I - and Topo IV -treated DNA IV showed a further decrease in the contour length by about 17% and 12%, respectively, compared to that of DNA IV. The shortening of DNA V and DNA VI was likely to be resulted from the condensation of DNA strands into the central node structure. The sizes of the DNA nodes in *Pst* I - and Topo IV -treated DNA IV

molecules were also compared. The mean diameter and height of the novel type of structure in the former molecules (~40.42 nm of the diameter and ~3.016 nm of the height) were both slightly larger than those in the latter (~38.51 nm of the diameter and ~2.779 nm of the height), which might explain why the former molecules showed a shorter contour length than the latter ones. Due to the highly compaction of the central node structures in both DNA V and DNA VI, it is hard to define the path of the DNA double strands in the structures. Therefore, further studies are needed to understand whether the central nodes in DNA V and DNA VI are knotted or not.

References

- [1] Vinograd J, Lebowitz J. Physical and topological properties of circular DNA. *J Gen Physiol*, 1966, **49**(6): 103-125
- [2] Huang X T, Chen X. Supercondensed structure of plasmid pBR322 DNA in an *Escherichia coli* DNA topoisomerase II mutant. *J Mol Biol*, 1990, **216**(2): 195-199
- [3] Drlaca K. Biology of bacterial deoxyribonucleic acid topoisomerases. *Microbiol Rev*, 1984, **48**(4): 273-289
- [4] Tsao Y P, Wu H Y, Liu L F. Transcription-driven supercoiling of DNA: direct biochemical evidence from *in vitro* studies. *Cell*, 1989, **56**(1): 111-118
- [5] Gotoh O. Prediction of melting profiles and local helix stability for sequenced DNA. *Adv Biophys*, 1983, **16**(1): 1-52
- [6] Leonard A C, Grimwade J E. Regulating DnaA complex assembly: it is time to fill the gaps. *Curr Opin Microbiol*, 2010, **13** (6): 766-772
- [7] Iftode C, Borowiec J A. Denaturation of the simian virus 40 origin of replication mediated by human replication protein A. *Mol Cell Biol*, 1997, **17**(7): 3876-3883
- [8] Vukojevic V, Yakovleva T, Terenius L, *et al.* Denaturation of dsDNA by p53: fluorescence correlation spectroscopy study. *Biochem Biophys Res Commun*, 2004, **316**(4): 1150-1155
- [9] Takahashi S, Motooka S, Usui T, *et al.* Direct single-molecule observations of local denaturation of a DNA double helix under a negative supercoil state. *Anal Chem*, 2015, **87**(6): 3490-3497
- [10] Pan B Y, Zhang L, Dou S X, *et al.* Forces-induced pinpoint denaturation of short DNA. *Biochem Biophys Res Commun*, 2009, **388**(1): 137-140
- [11] Hanke A. Denaturation transition of stretched DNA. *Biochem Soc Trans*, 2013, **41**(2): 639-645
- [12] Yan L, Iwasaki H. Thermal denaturation of plasmid DNA observed by atomic force microscopy. *Japanese Journal of Applied Physics*, 2002, **41**(12R): 7556-7559
- [13] Yu J, Zhang Z, Cao K, *et al.* Visualization of alkali-denatured supercoiled plasmid DNA by atomic force microscopy. *Biochem Biophys Res Commun*, 2008, **374**(3): 415-418
- [14] Jansz H S, Baas P D, Pouwels P H, *et al.* Structure of the replicative form of bacteriophage phi X174. V. Interconversions between twisted, extended and randomly coiled forms of cyclic DNA. *J Mol Biol*, 1968, **32**(2): 159-168
- [15] Pouwels P H, Knijnenburg C M, Van Rotterdam J, *et al.* Structure of the replicative form of bacteriophage phi X174. VI. Studies on alkali-denatured double-stranded phi X DNA. *J Mol Biol*, 1968, **32**(2): 169-182
- [16] Strider W, Camien M N, Warner R C. Renaturation of denatured, covalently closed circular DNA. *J Biol Chem*, 1981, **256** (15): 7820-7829
- [17] Grossman L I, Watson R, Vinograd J. Restricted uptake of ethidium bromide and propidium diiodide by denatured closed circular DNA in buoyant cesium chloride. *J Mol Biol*, 1974, **86**(2): 271-283.
- [18] Johnson P H, Miller M J, Wild E, *et al.* Electrophoretic characterization of intracellular forms of bacteriophage phi X174 DNA: identification of novel intermediate of altered superhelix density. *J Virol*, 1979, **32**(2): 629-639
- [19] Kato J, Suzuki H, Ikeda H. Purification and characterization of DNA topoisomerase IV in *Escherichia coli*. *J Biol Chem*, 1992, **267**(36): 25676-25684
- [20] Lopez V, Martinez-Robles M L, Hernandez P, *et al.* Topo IV is the topoisomerase that knots and unknots sister duplexes during DNA replication. *Nucleic Acids Research*, 2012, **40**(8): 3563-3573
- [21] Rybenkov V V, Ullsperger C, Vologodskii A V, *et al.* Simplification of DNA topology below equilibrium values by type II topoisomerases. *Science*, 1997, **277**(5326): 690-693
- [22] Deibler R W, Rahmati S, Zechiedrich E L. Topoisomerase IV, alone, unknots DNA in *E. coli*. *Genes Dev*, 2001, **15**(6): 748-761
- [23] Peng H, Marians K J. The interaction of *Escherichia coli* topoisomerase IV with DNA. *J Biol Chem*, 1995, **270**(42): 25286-25290
- [24] Orphanides G, Maxwell A. Evidence for a conformational change in the DNA gyrase-DNA complex from hydroxyl radical footprinting. *Nucleic Acids Res*, 1994, **22**(9): 1567-1575

DNA 双链区的切割导致碱变性超螺旋质粒 pBR322 的分子内结节*

田 磊¹⁾ 苏小运²⁾ 张臻峰^{3)**} 黄熙泰⁴⁾

¹⁾ 中国人民解放军海军总医院普外科, 北京 100048; ²⁾ 中国农业科学院饲料研究所, 北京 100081;

³⁾ 中国科学院微生物研究所微生物资源前期开发国家重点实验室, 北京 100101; ⁴⁾ 南开大学生命科学学院, 天津 300071)

摘要 为进一步研究碱变性超螺旋 DNA(IV 型 DNA; DNA IV) 的结构, 对碱变性质粒 pBR322 进行了酶学分析并利用原子力显微镜(AFM)对新形成的 DNA 结构进行了观察和比较. 在所有已检测的限制酶中只有 *Pst* I 可以切割质粒 pBR322 的 IV 型 DNA 分子, 说明在这种变性的 DNA 分子中仍存在少数完整的限制酶识别位点. 与碱变性 DNA 分子的闭合环状结构相反, AFM 成像的结果显示 *Pst* I 处理后的 DNA IV 分子均为开放结构, 同时这种分子包含明显的 DNA 结节. 与 DNA IV 分子相比, 这种 DNA 分子的表现长度缩短了大约 11%. 有意思的是, 大肠杆菌拓扑异构酶 IV (一种 II 型拓扑异构酶) 也可以在 pBR322 DNA IV 分子中引入分子内结节, 而这种结节 DNA 分子仍然保持闭合状态. AFM 的结果表明上述两种结节的 DNA 分子在表现长度及结节结构的尺寸上均比较相似. 这些发现证实, 在碱变性的超螺旋 DNA 分子中仍然保留着一些长度较短的、含有特异性碱基配对的 DNA 双链区, 而在这些区域内的 DNA 双链断裂可以导致 DNA 结节.

关键词 DNA IV, 限制性内切酶, DNA 拓扑异构酶, DNA 结节, 原子力显微镜

学科分类号 Q5, Q6, Q7, Q93

DOI: 10.16476/j.pibb.2015.0160

* 国家自然科学基金资助项目(31270124, 30900023).

** 通讯联系人.

Tel: 010-64807418, E-mail: zhangzf@im.ac.cn

收稿日期: 2016-04-05, 接受日期: 2016-05-16